

High-Quality Free-standing GaN Thick-films Prepared by Hydride Vapor Phase Epitaxy using Stress Reducing Techniques

Hsin-Hsiung Huang^a, Wei-I Lee^{a,d}, Kuei-Ming Chen^{a,b}, Ting-Li Chu^a, Pei-Lun Wu^a, Hung-Wei Yu^a, Po-Chun Liu^b, Chu-Li Chao^b, Tung-Wei Chi^b, Jenq-Dar Tsay^b, and Li-Wei Tu^c

^a *Department of Electrophysics, National Chiao Tung University, Hsinchu, Taiwan, ROC*

^b *Industrial Technology Research Institute, Hsinchu, Taiwan, ROC*

^c *Department of Physics and Center for Nanoscience and Nanotechnology, National Sun Yat-Sen University, Kaohsiung, Taiwan, ROC*

ABSTRACT

As one of the most mature techniques for manufacturing free-standing GaN substrates, hydride vapor phase epitaxy (HVPE) always encounters problems associated with residue thermal stress, such as GaN bending and cracking during and after growth. This work presents a patterning approach and a non-patterning approach to reduce stress in thick GaN films grown on sapphires by HVPE. The patterning approach, forming dot air-bridged structures, adopted standard photolithography to fabricate hexagonally aligned patterns of dots on GaN templates. Following HVPE growth, regular voids were formed and buried in the GaN thick-films. These voids helped to relax the stress in the GaN thick-films. In the non-patterning approach, thick GaN films were simply grown at a specially set sequence of ramping temperatures during HVPE growth without any patterned structure. This temperature-ramping technique, gives crack-free high-quality 2"-diameter GaN films, thicker than 250 μm , on sapphires in high yields. These thick GaN films can be separated from sapphire using conventional laser-induced lift-off processes, which can be followed by subsequent HVPE regrowths. A 600 μm -thick free-standing GaN films has a typical dislocation density of around $4 \times 10^6 \text{ cm}^{-2}$ with a full width at half maximum (FWHM) in the high resolution X-ray diffraction (HRXRD) spectrum of GaN (002) of around 150 arcsec.

The residual stress in the thick GaN films was analyzed by micro-Raman spectroscopy. The effectiveness of the patterning and the non-patterning techniques in reducing the strain in GaN films is discussed. The advantages and weaknesses of the patterning and the non-patterning techniques will be elucidated.

Keywords: HVPE, GaN, LLO, freestanding , residual stress

^d contact author, email : wilee@mail.nctu.edu.tw

1. Introduction

GaN and its related alloys have attracted much interest in recent decades because of their wide bandgaps, excellent physical properties and chemical stability. GaN devices, such as light emitting diodes (LEDs), field effect transistors (FETs) and laser diodes (LD), have many a range of applications, such as in traffic lights, full-color displays, and others. Given the difficulty of obtaining high-quality GaN substrates, most current nitride-based devices are hetero-epitaxially grown on lattice-mismatched substrates, such as sapphire, Si, GaAs, and SiC. The large mismatches between the lattice constants of substrates and epitaxial films yield high dislocation densities. Additionally, differences between the thermal expansion coefficients (TEC) of the substrates and the epitaxial films cause large warping or bowing of the epi-layers.

Many approaches to GaN substrate growth have been proposed. They include, Na flux, N₂ high pressure growth, ammonothermal, and HVPE. The N₂ high pressure growth approach grows GaN bulk of excellent quality, but of small size and at a low growth rate, which limits the range of commercial applications. Dwiliński *et al.* produced high-quality GaN bulk of large size using the ammonothermal method. However, the rate of low growth of GaN bulk by the ammonothermal approach makes obtaining GaN substrate economically very difficult. [1] The HVPE technique provides a high growth rate and a high-quality GaN substrate. However, it is associated with some problems that still need to be solved, including the cracking caused by the difference between the TEC of the GaN and the foreign substrate, warping, and lift-off of the foreign substrate.

In this work, an HVPE system was adopted to study the fabrication of GaN wafer. Approaches to prevent the cracking of GaN thick-films during the HVPE epitaxy process were adopted herein this work, including the air-bridged, dot air-bridged, and temperature ramping techniques. These methods effectively prevent cracking of the GaN thick-film during the HVPE growth process. After the GaN thick-film had been prepared, the laser lift-off approach was adopted to separate the GaN thick-film from the original substrate. A freestanding GaN thick-film was thus obtained. Its characteristics were analyzed by SEM, CL, Raman spectroscopy, PL, Hall measurement, HRXRD, AFM, and Normaski OM.

Freestanding GaN with a thickness more than 360 μm was obtained using the strain-reduced methods. It was transparent and its dislocation density was in the range 10⁶ to 10⁷ cm⁻². The resistivity was about 0.09 Ω-cm. The undoped carrier concentration was about 1.6x10¹⁷ cm⁻³. The FWHM of the HRXRD rocking curve was about 120 arcsec.

2. Air-Bridged and Dot Air-Bridged Epitaxial Lateral Overgrowth

Selective epitaxial approaches, such as lateral epitaxial overgrowth (LEO) and pendeo epitaxy (PE) have been demonstrated to be highly effective in reducing the density of threading dislocations (TDs) by over two orders of magnitude in two to several steps of the lateral growth of GaN films on sapphire and SiC substrates. [2-5] However, c-axis tilting in the wing region of commonly 0.2°-1° is typically observed in both LEO and pendeo structures azimuthally perpendicular to the LEO or PE stripe. When wing tilt is present, the coalescence of nearby stripes may yield arrays of dislocations, reducing the defect-free region of overgrown GaN. [6] Kidoguchi *et al.* proposed a new method of lateral growth, called air-bridged LEO, which improves on the wing tilting caused by conventional selective epitaxy. [7-9] Dry etching and standard photolithography were adopted herein to form trenches in a GaN template, and the sidewall of the GaN trenches was covered with a dielectric mask, such as SiN_x or SiO₂, in an air-bridged LEO structure. After GaN had regrown, the voids in the air-bridged structure were buried in the coalesced GaN wings. However, the effect of the height of voids in an air-bridged structure is currently not clearly understood, especially in relation to the distribution of stress that is generated by the difference between the TECs of the epitaxial films and the substrate in thick GaN films.

In this work, a novel air-bridged structure with high voids was designed to grow thick GaN layers by HVPE. The quality of the GaN layers grown in this way using this approach was compared to that of GaN layers that had been prepared by a more conventional pendeo growth process with lower voids. The HVAB structure with the higher voids reduces the density of TDs and the residual stress induced by the difference between TECs, and to yield a self-separated freestanding GaN wafer from the sapphire substrate. [10]

To provide a meaningful comparison, a 4 μm-thick GaN layer was initially grown on a c-plane sapphire substrate by metal-organic chemical vapor deposition (MOCVD). Then, a standard photolithographic approach was adopted to fabricate a pattern of 4 μm-wide GaN seed stripes and 6 μm-wide grooves between adjacent stripes in the (1-100) direction of GaN. Trenches were dry-etched to a depth of 0.2 μm into the sapphire. The GaN template was then sliced into two half-wafers. One of the half-wafers (pendeo structure) remained without any additional treatment. The other half-wafer (HVAB structure) was passivated using a thin oxide layer on the sidewall of the GaN seed. The two half-wafers were then mounted side by side in an HVPE reactor to grow 30 μm GaN. Figures. 1(a) and (c) schematically

depict the conventional pendeo and the HVAB structures, respectively, following the HVPE regrowth which involved the use of NH_3 gas as a nitrogen source and GaCl, generated at 850 °C from liquid gallium with HCl gas, as a gallium source. The ambient of the carrier gas was a mixture of H_2 and N_2 . The growth was proceeded in an AIXTRON 800064 horizontal reactor at about 1050 °C. The GaN growth comprised two steps at different pressures; the first step was lateral overgrowth at 500 mbar and the second step was 3D growth at 900 mbar.

Figures 1(b) and (d) present cross-sectional SEM images of the GaN films formed from conventional pendeo and HVAB structures. Conventional pendeo and HVAB structures contain voids of various heights under HVPE GaN at the coalescence boundary of the wing region; neither structure contains small tapered voids. The heights of the voids in the pendeo and the HVAB structures are 0.2 and 3 μm , respectively. The heights of the voids in the HVAB structure markedly exceeds that of those in the conventional air-bridged LEO. [7-9]

Figure 2 presents cross-sectional and plane-view CL images of conventional pendeo and HVAB structures. The cross-sectional CL images in Figs. 2(a) and 2(c) elucidate the GaN growth mechanism of pendeo and HVAB structures. The bright region in images of the the conventional pendeo and HVAB structures is the selective epitaxial growth region. TDs are more likely to propagate to the GaN surface in the conventional pendeo structure than in the HVAB structure in the seed region. Figures 2(b) and (d) present the plane-view CL images of conventional pendeo and HVAB structures. The density of TDs in the GaN surface can be determined from the CL image. On both samples, most of the TDs were confined in the coalescence region. However, the dislocation density in the sample with the HVAB structure sample was much lower than that in the sample with the conventional pendeo structure. EPD measurements supported similar conclusion. The densities of TDs in HVAB and conventional pendeo structures in the wing region are about 10^7 and 10^8 cm^{-2} , respectively. In another experiment, the width of the grooves in the HVAB structure is increased to over 10 μm , the density of TDs is reduced to 10^6 cm^{-2} in the wing region.

Figure 3 schematically depicts the propagation of TDs in conventional pendeo and HVAB structures. Since the sidewalls of GaN seeds were passivated with oxide in the HVAB structure, the regrowth of GaN by HVPE could began only at the top of the GaN seeds, forming triangular ELOG GaN in the initial stage of regrowth. The TDs were thus then more likely to bend and coalesce. In conventional pendeo regrowth, the sidewalls of the GaN seeds did not exhibit passivation and, therefore, the GaN began to grow from the sidewall as well as from the top, rapidly coalescing immediately above the groove region. The TDs were not able to have enough opportunity to coalesce and propagated to the surface of the GaN thick film.

The measured X-ray rocking curve of either conventional pendeo or HVAB structures in 30- μm -thick GaN films provide no clear evidence of wing tilt. The FWHM of the GaN symmetric (002) and asymmetric (102) peaks of the HRXRD rocking curves are 202 and 204 arcsec, respectively, which are better than those of the conventional pendeo. The result that thick GaN films can reduce wing tilt is consistent with the study of Ishibashi *et al.*[10] The wing tilt produces stress in the coalescent region, which disfavors the growth of high-quality GaN thick films by HVPE. The FWHM of (002) and (102) X-ray rocking curves show the high quality of the samples in both conventional pendeo and HVAB structures. The FWHM of the (102) peak is broadened by screw, mixed, and edge dislocations.[11, 12] The FWHM value of the HVAB GaN (102) peak in the rocking curve, as low as 204 arcsec indicates that the number of all types TDs is reduced in the HVAB structure, even in the direction of lateral overgrowth.

The residual strain of these samples was measured by micro-Raman scattering spectroscopy with the $\text{E}_2(\text{high})$ phonon frequency. Figure 4 presents the cross-sectional and in-plane Raman spectra of conventional pendeo and HVAB structures. The difference between the TECs of GaN and sapphire substrate produces compressive stress that is commonly observed in the GaN film upon hetero-epitaxial growth on the sapphire substrate. Given an $\text{E}_2(\text{high})$ mode phonon wavenumber of 567.0 cm^{-1} as the reference value for strain-free GaN, a blue-shift of the Raman $\text{E}_2(\text{high})$ mode of 4.24 cm^{-1} would correspond to a stress of 1 GPa.[13, 14] The compressive stress in the surface of the HVAB structure is 165 MPa less than that in the conventional pendeo structure, above both the window and the wing regions, and this value is similar to that in the cross-sectional region of these samples. Therefore, the relaxation of residual stress in the HVAB structure exceeds that in the conventional pendeo structure.

The growth mechanism of the high-void air-bridged structure differs from that of the conventional pendeo structure because of the generation of high voids by the sidewall passivation of the GaN seed. CL, HRXRD, EPD, and Raman spectra show that the HVAB growth process markedly improves GaN quality. The relaxation of the residual stress of the HVAB structure exceeds that of the conventional pendeo structure, which factor is important in the growth of a GaN thick film by HVPE. However, the HVAB structure still has a disadvantageous residual stress distribution, which differs between the x and y directions because of the patterned stripes. For advanced controlling of the distribution of stress, an especially designed two-dimensional pattern, called the dot air-bridged structure was developed for growing thick GaN layers using an HVPE system.

Figure 5 presents the growth of dot air-bridged structures by HVPE. The photolithography steps of the fabrication process are similar to those in fabricating the HVAB structure. The difference between the HVAB structure and the dot air-bridged structure is that the seeds of the HVAB structure are one-dimensional stripes but the seeds of dot air-bridged structure are a two-dimensional hexagonally aligned pattern of 3 μm -wide square seed regions, which are separated by 4 μm -wide grooves. The sample was mounted in the HVPE reactor to grow GaN thick-film, as presented in Fig. 5(d).

NH_3 gas was used as a nitrogen source and GaCl generated from liquid gallium and HCl gas at 850 $^\circ\text{C}$ was used as a gallium source in the HVPE growth of the GaN thick-film in an Aixtron 800064 horizontal reactor at about 1050 $^\circ\text{C}$ and 900 mbar pressure, in a mixed of H_2 and N_2 ambient.

Figure 6(a) presents an SEM image of the GaN template of the dot air-bridged structure before the HVPE growth of the GaN thick-film. The sidewall of GaN seeds was passivated using a very thin SiO_2 layer and isolated in a hexagonal array. Figure 6(b) presents the SEM image following the initial 10 min of growth by HVPE. The GaN seed region formed a pyramid shape with (10-11) crystal facets, which were easily observed following GaN growth. The properties and the fill factor of the grooves and seeds of the dot air-bridged structure will be presented in the future. Figure 7 presents the plane view CL image of the dot air-bridged structure following the HVPE growth of the GaN thick-film. The dark spots show that the density of dislocations in GaN with the dot air-bridged structure was about $2 \times 10^7 \text{ cm}^{-2}$, which is one to two orders lower than that in GaN grow directly on sapphire substrate without any designed pattern.

The samples grown with dot air-bridged structure were transparent and entirely free of cracks, indicating that the residual stress was effectively eliminated in the dot air-bridged GaN. A freestanding GaN wafer was fabricated (using the subsequent laser lift-off (LLO) approach).

To understand the distribution of residual stress in the deep parts of the dot air-bridged GaN thick-film, a 100 μm -thick GaN sample that remained on sapphire substrate was cleaved to measure the stress variation along the cross-section. The stress was measured by micro-Raman spectroscopy in the $\text{E}_2(\text{high})$ phonon mode. Different regions of the cross-sectional dot air-bridged GaN - the bottom, the middle and the top - were studied by micro-Raman spectroscopy.

The stress of the dot air-bridged sample upon the interface was 0.04 GPa in compression, which was calculated by taking the $\text{E}_2(\text{high})$ mode phonon frequency at 567.0 cm^{-1} as the reference value for strain-free GaN. [15] The stress is much smaller than that standard ELOG samples and GaN grown directly on sapphire substrate.[16, 17]

Figure 8(a) presents a photograph of a 1.5 inch-diameter GaN thick-film with a thickness of 300 μm on 2 inch sapphire substrate. The surface of the GaN thick-film was mirror-like and no crack was observed on either the GaN thick-film or the sapphire substrate. Figure 8(b) presents a photograph of the freestanding GaN wafer from the sample in Fig. 8(a), which was separated from the sapphire substrate by the LLO approach.

The crack-free GaN thick-film with a diameter of 1.5 inch and a thickness of 300 μm with the dot air-bridged structure, was formed by HVPE and LLO approaches. The dislocation density was about $2 \times 10^7 \text{ cm}^{-2}$ and the residual stress of the dot air-bridged structure was reduced to as low as 0.4 GPa, preventing the crack of GaN and sapphire in the epitaxial process. The dot air-bridged approach can be used to fabricate large-area crack-free GaN thick-films, which are required for the manufacture of GaN substrate.

3. Temperature Ramping Technique

When GaN is grown by HVPE, a sapphire substrate is typically used as a foreign substrate, because of its reliability and low cost. The 16% lattice mismatch and the $2 \times 10^{-6}/\text{K}$ difference between the TECs of sapphire and GaN always cause cracking of the GaN and sapphire.[18-20]

Many approaches that exploit the self-separation method have been developed for producing freestanding GaN thick films by HVPE. They include void-assisted separation, facet-controlled separation, and WSiN_x epitaxial lateral overgrowth approaches.[21-24] These self-separation techniques can produce crack-free GaN thick-films. However, their yield of complete freestanding GaN wafers without any cracks remains very low.

In this experiment, a very simple approach involved no complex process was adopted to prevent cracks in the HVPE growth of GaN thick-film. Large-area, thick freestanding GaN films were thus produced.

First, a 4- μm -thick MOCVD GaN layer was prepared on a c-plane sapphire substrate as a template for the HVPE regrowth of the GaN thick-film. The MOCVD GaN template was mounted in a horizontal HVPE reactor. The HVPE GaN growth was began at a low temperature (LT), 950 $^\circ\text{C}$, and continued for 30 min; then, the temperature was ramped to a high temperature (HT) of 1050 $^\circ\text{C}$ at a ramping rate of about 1 $^\circ\text{C}/\text{min}$. Following the ramping process, the HVPE growth temperature of the GaN was maintained at 1050 $^\circ\text{C}$ until the thickness reached 360 μm . The conditions for the HVPE growth of GaN were the same as those for HVAB and dot air-bridged structures but the pressure was maintained at 900 mbar throughout the growth process.

Figure 9 presents the full structure of the GaN film grown using the temperature ramping technique. The thickness of GaN layer grown at 950 °C (LT) by HVPE was about 50 μm. The thicknesses of the GaN films grown using with temperature ramping and at HT were about 130 μm and over 180 μm, respectively.

As the photography in Fig. 10(a) presents, the sample grown with temperature ramping has the transparent, crack-free and mirrorlike surface properties. However, the sample grown without temperature ramping and LT layer was cracked. The crack-free GaN layer with a thickness of 360 μm and a 2 inch diameter was separated from the sapphire substrate by an LLO using a 355 nm Nd:YAG laser, as presented in Fig. 10(b). The radius of curvature radius of the GaN wafer was about 0.4 m before lift-off from the sapphire substrate; that of the freestanding GaN wafer following LLO from the sapphire substrate exceeded 2 m. The ring of the outer was caused by the high power density of the laser pulse.

In the LLO process, the GaN layer is separated from the substrate by irradiating the substrate-film interface with a high-power laser pulse through the substrate at a wavelength that can be transmitted. The sapphire substrate is the most suitable substrate for use with the LLO approach. The absorption of the laser pulse energy by GaN in the LLO process causes rapid thermal decomposition of the irradiated GaN interfacial layer into gaseous N₂ and metallic Ga.

High-intensity laser pulses enter the GaN/sapphire interface through the side of the sapphire. The shock wave decomposes the thin GaN layer. The samples are placed on sapphire powder to dampen the laser pulse. An additional hot plate is adopted to increase the temperature to relax the bowing that is caused by the difference between the TECs of GaN and the substrate during the LLO process. The most suitable laser systems in the case of GaN/sapphire are the third harmonic of the Q-switch Nd:YAG laser and the excimer KrF laser.[25-127] The wavelengths of the GaN/sapphire LLO of Nd:YAG and KrF lasers are 355 and 248 nm, respectively. In this experiment, the chosen laser system is an Nd:YAG 355 nm laser.

The HVPE GaN was characterized by SEM, CL measurement, HRXRD analysis, micro-Raman spectroscopy, and etch pit density (EPD) measurement. The EPD conditions were 220 °C for 20 min in a mixture of H₃PO₄ and H₂SO₄ in a ratio of 1:3. To understand the residual stress distribution, CL and Raman measurements were made on another cleaved 300 μm-thick GaN film without separating it from the sapphire substrate.

The Raman scattering spectra were obtained from the bottom, middle and top regions of the cross-sectional sample. The middle and top regions corresponded to the ramping layer and the HT growth layer, respectively. Figure 11 presents the result of Raman scattering spectra.

The peaks of the E₂(high) mode phonon frequency were used to calculate the residual stress in the bottom, ramping, and HT regions, which corresponded to compressive stresses of 0.12, 0.12, and 0.07 GPa, respectively. The residual stress of the sample was grown without ramping and LT layers was calculated in the bottom region of GaN; it was a compressive stress of 0.5 GPa, which was much larger than that of the samples with LT and ramping steps.

The low-temperature (15 K) CL spectra of a cross-section region were also obtained at the same position as Raman spectra. Near-band-edge emission peaks were observed at 358 nm, 358 nm, and 357 nm, corresponding to the bottom, ramping, and HT regions, respectively, in HVPE GaN. The residual stress was calculated with reference to the strain-free emission peak at 3.467 eV.[28] The bottom and ramping regions had a small tensile stress of 0.1 GPa, which was consistent with that determined from the Raman spectrum.

The residual stress was calculated from the CL and Raman spectra. It was less in GaN thick-films that were grown on sapphire substrates using the temperature ramping technique. The relaxation of thermal stress is very important in preventing the crack of the GaN thick-film that is grown on a sapphire or other substrate. This technique can be adopted to fabricate GaN substrates by HVPE. The LT and temperature ramping layers acted as a large buffer layer, which relaxed the residual stress and thus prevented crack of the GaN thick films that were grown on the sapphire substrate.

Figure 12 presents the FWHM of the HRXRD rocking curve of the (002) GaN before and after the LLO process. Before LLO, the FWHM of GaN (002) exceeded 800 arcsec because of the warping of the GaN/sapphire structure. After LLO, the FWHM of the freestanding GaN thick-film was relaxed to 150 arcsec. The more detail of the results were published in previous paper.[A]

Figure 13(a) presents a plane-view CL image of the 300 μm-thick free-standing GaN. The dislocation density is about 1×10⁷ cm⁻² calculated from both the CL image and the EPD measurement. Figure 13(b) presents the CL image of the regrown GaN thick-film with a thickness of about 600 μm. The dislocation density is reduced to 4×10⁶ cm⁻², indicating that increasing the GaN thickness can reduce the dislocation density.

Figure 14 presents the Raman spectra of a GaN thick-film before and after the LLO process. The stress was analyzed by examining the E₂(high) phonon mode of the Raman spectrum. The E₂(high) mode of the GaN thick-film after the LLO process is shifted by 0.5 cm⁻¹ shift from that before the process, indicating that 120 mPa of compressive stress in the top of the GaN thick-film was relieved after the LLO process. The stress of the GaN thick-film on sapphire was much less than that of the GaN thin-film on sapphire, but the LLO process relieved more of the residual stress.

A very simple technique for preventing crack of GaN thick-films that are grown by HVPE without any complex photolithographic or other process is developed. High-quality freestanding GaN films with thicknesses of over 300 μm and diameters of 2 inch can be produced using this technique after a subsequent LLO process.

4. Conclusion

In the last decade, the saving of energy and the reduction of carbon output have attracted much interest because of both the effects on global warming and the inflation of the cost of energy. GaN and its related materials are important in saving energy, such as when they are used in solid state lighting. However, lattice-matched substrates are lacking and so most nitride-based devices are currently hetero-epitaxially grown on lattice-mismatched substrates. Large mismatches between the lattice constants of the substrates and the epitaxial films cause high defect densities. Additionally, differences between the thermal expansion coefficients of substrates and epitaxial films cause extensive warping or bowing of the epi-layers.

In this work, freestanding GaN wafers were developed to fabricate GaN substrate to solve the aforementioned problems. Many structures and techniques were adopted to relieve thermal stress and eliminate crack as follows.

- 1、 An HVAB structure GaN thick-film was developed and discussed. The growth mechanism of the HVAB structure differs from that of the conventional pendeo structure because of the formation of high voids by the sidewall passivation of the GaN seed. CL, HRXRD, EPD, and Raman spectra show that the HVAB growth process markedly improves GaN quality. The relaxation of the residual stress in the HVAB structure exceeds that of the conventional pendeo structure.
- 2、 To eliminate the disadvantages of a striped air-bridged structure and to relax the thermal stress, a strain-reduced structure called a dot air-bridged structure was developed for growing GaN thick-film by HVPE. The compressive stress was reduced to as low as 0.04 GPa to prevent cracking during the epitaxial GaN growth. This approach yielded a large-area GaN thick-film, which was adopted to fabricate a freestanding GaN wafer.
- 3、 A very simple temperature ramping technique for preventing the cracking of a GaN thick-film grown by HVPE with no complicated process is developed. High-quality 2 inch-diameter large-area freestanding GaN layers with a thickness of over 300 μm was thus obtained by LLO process. The FWHM of the HRXRD of GaN (002) was about 150 arcsec and the dislocation density was about 1×10^7 to $4 \times 10^6 \text{ cm}^{-2}$. No additional designed-patterned structure in these samples was required to reduce the dislocation density or thermal stress.

Acknowledgements

The authors would like to thank the National Science Council, under Contract No. NSC 97-2622-E-009 -002, and the Ministry of education of the Republic of China, Taiwan, under the MOEATU program, for financially supporting this research.

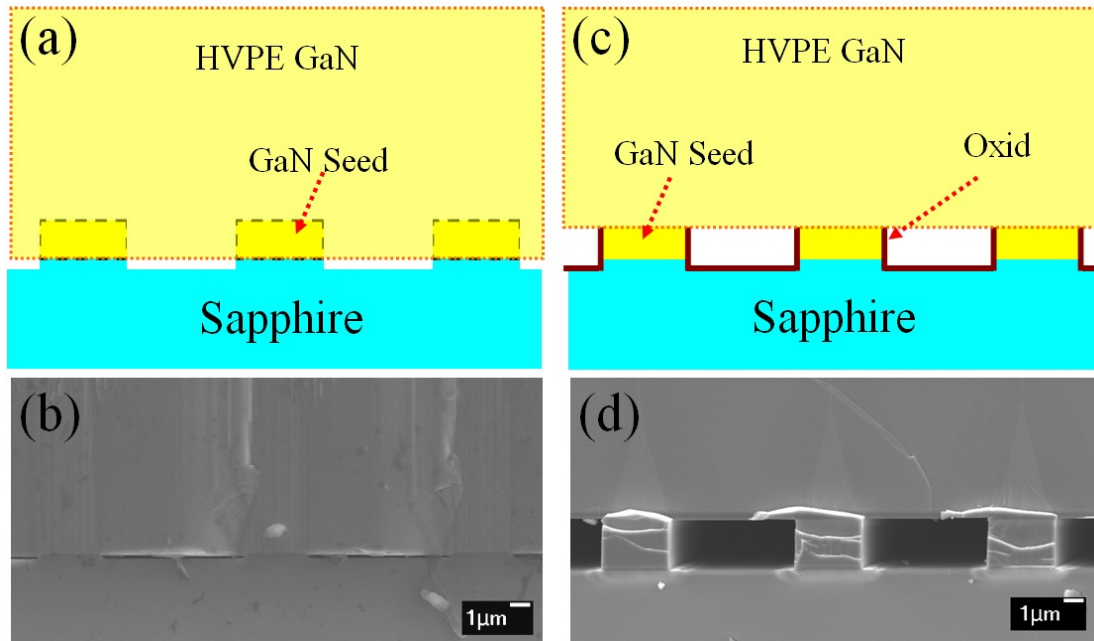


Fig. 1 Schematics and SEM images of the conventional pendeo and the HVAB structures after HVPE regrowth. (a) Schematic of the conventional pendeo structure. (b) SEM image of (a) after the HVPE regrowth. (c) Schematic of the HVAB structure. (d) SEM image of (c) after the HVPE regrowth.

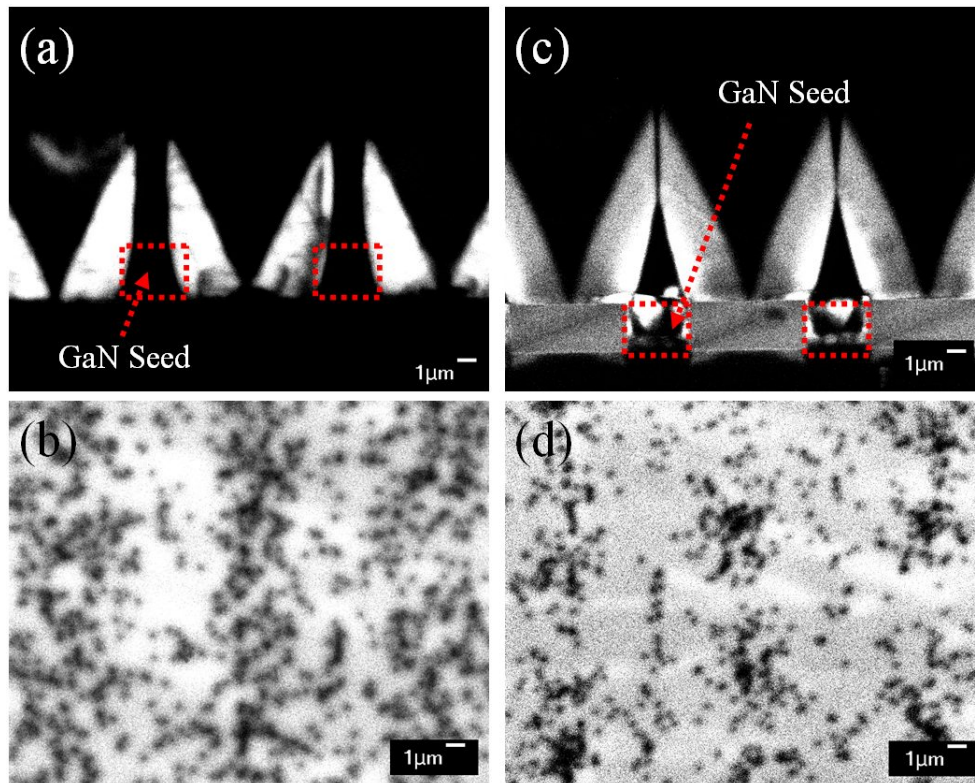


Fig. 2 Plane and cross-sectional CL images of the conventional pendeo and the HVAB structures. (a) Cross-sectional image of the conventional pendeo structure. (b) Plane-view of the conventional pendeo structure. (c) Cross-sectional image of the HVAB structure. (d) Plane-view of the HVAB structure.

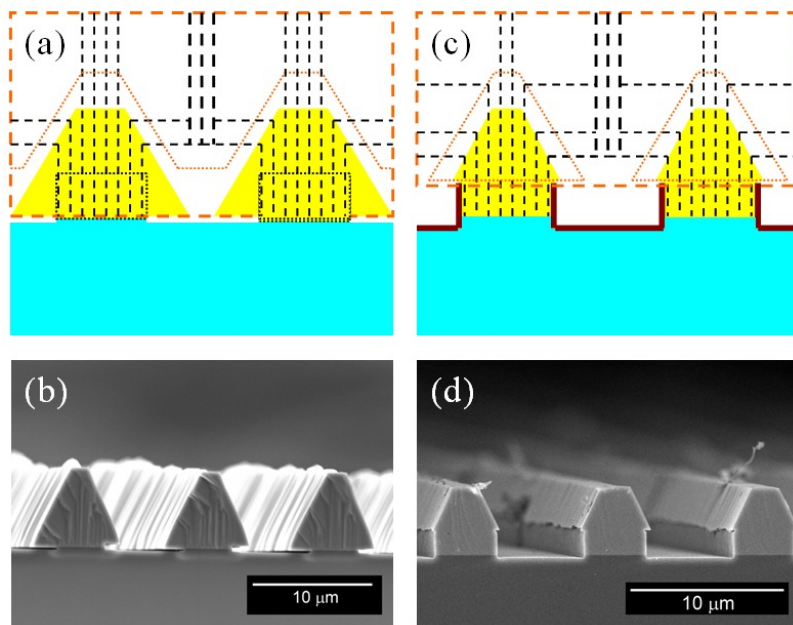


Fig. 3 Schematics of growth mechanism and SEM images of initial state of the HVPE regrowth in the conventional pendeo structure and the HVAB structures. (a) Schematic growth mechanism of the conventional pendeo structure. (b) Schematic of growth of the conventional pendeo structure. (c) SEM image of the initial growth of the HVAB structure. (d) SEM image of the initial growth of the HVAB structure.

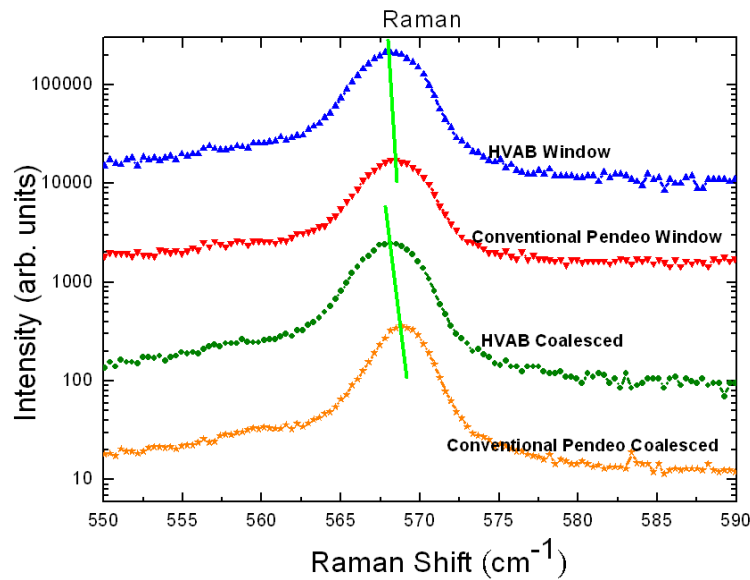


Fig. 4 Raman spectra of $E_2(\text{high})$ phonon frequency of the conventional pendeo and the HVAB structures in window and in wing regions.

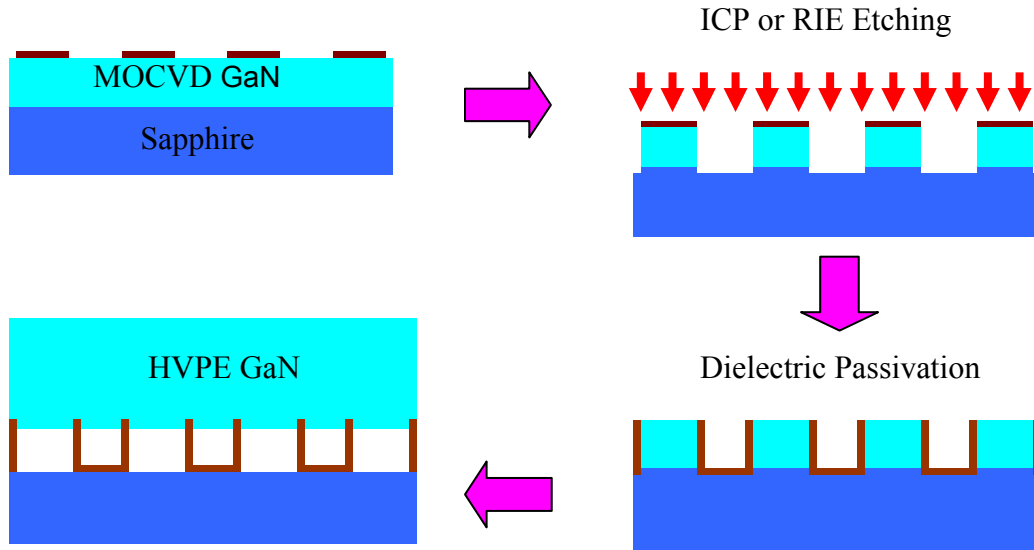


Fig. 5 Schematic of the GaN thick-film fabrication process with the dot air-bridged structure by HVPE. (a) MOCVD GaN template with SiNx hard mask. (b) Dry etching process by ICP. (c) The sidewall passivation of GaN seed regions. (d) GaN thick-film regrowth by HVPE.

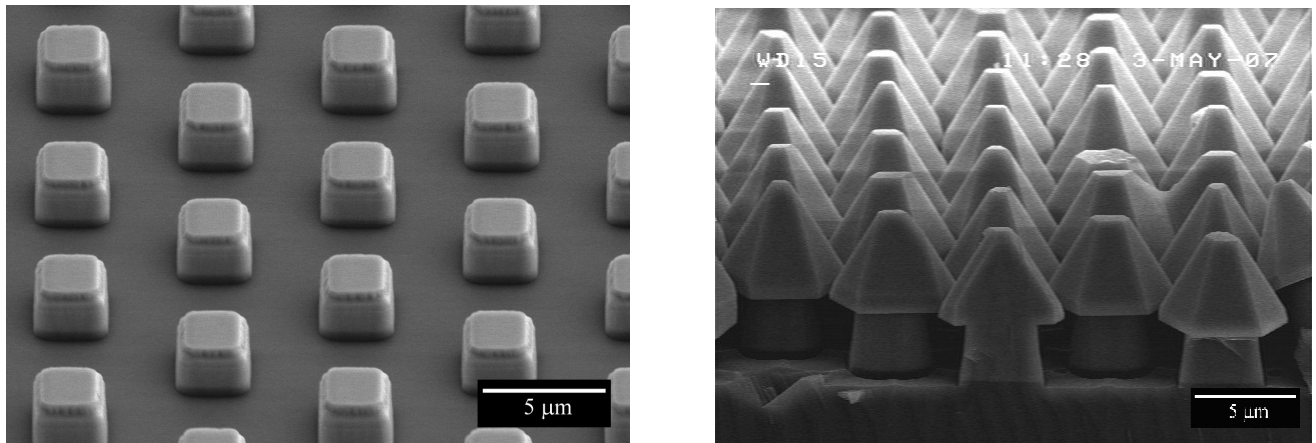


Fig. 6 (a) The bird's-eye view SEM image of the dot air-bridged structure. (b) The SEM image of 10 min initial growth state of the dot air-bridged structure by HVPE.

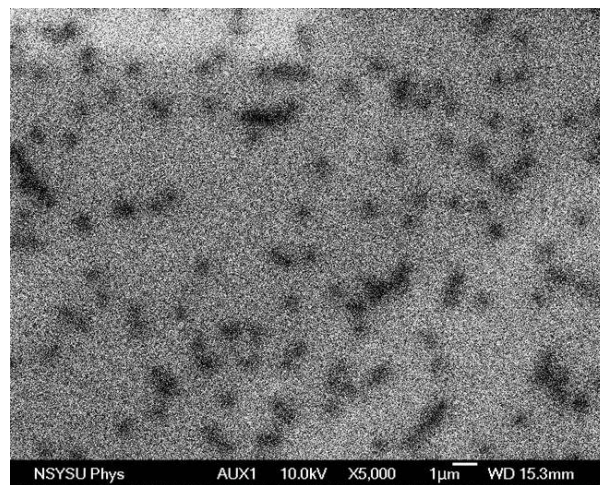


Fig. 7 The plane view CL image of GaN thick-film of the dot air-bridged structure by HVPE.

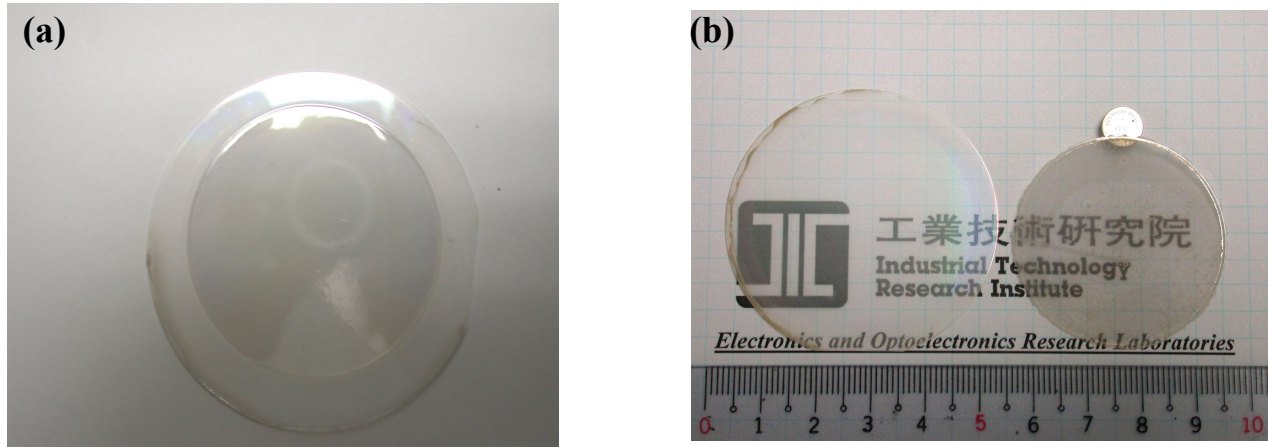


Fig. 8 (a) A 300 μm GaN thick-film in 1.5-inch diameter on 2-inch sapphire substrate without any crack. (b) The 300 μm freestanding GaN wafer in 1.5-inch diameter without any crack. The GaN wafer is transparent.

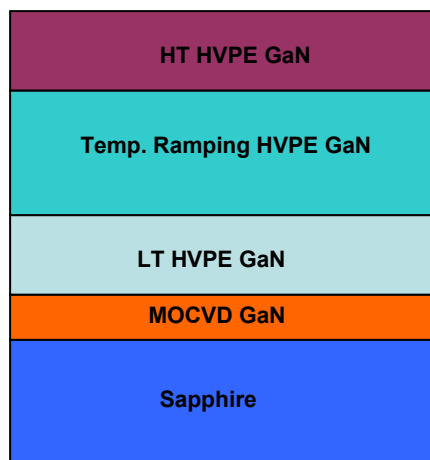


Fig. 9 Schematic of the temperature ramping GaN growth structure by HVPE.

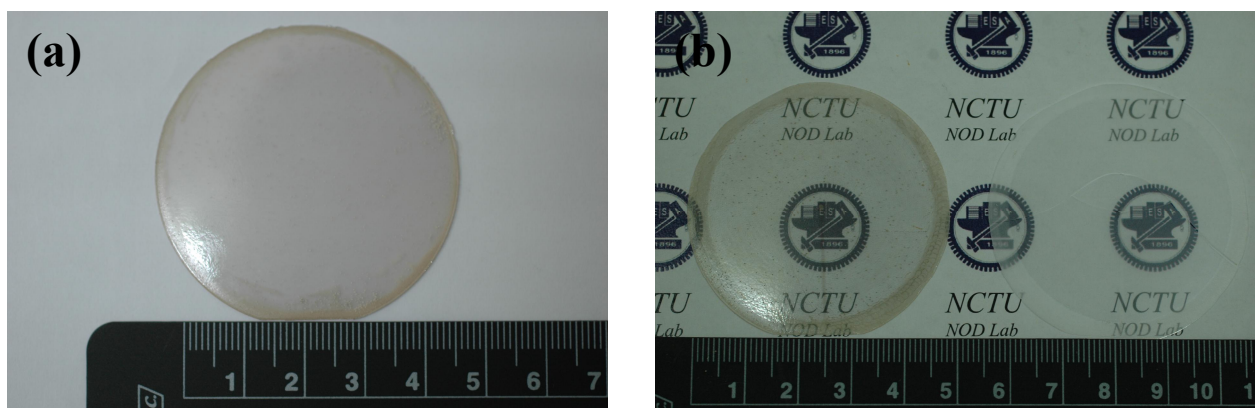


Fig. 10 (a) A 2 inch, 360 μm -thick GaN on sapphire substrate before LLO process. (b) Freestanding GaN wafer from (a) after the LLO process. The right hand side is the sapphire substrate and the left hand side is the GaN wafer.

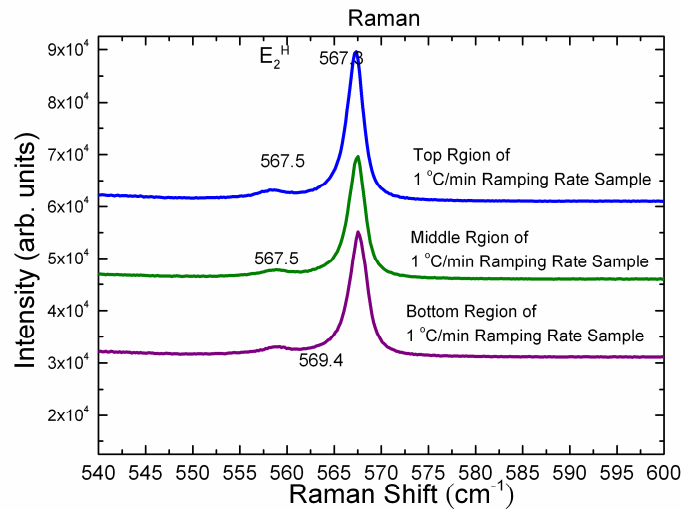


Fig. 11 The Raman spectra of cross-sectional regions of the same sample with 1.0 °C/min ramping rate. The spectra were measured at the bottom, the ramping, and the HT regions.

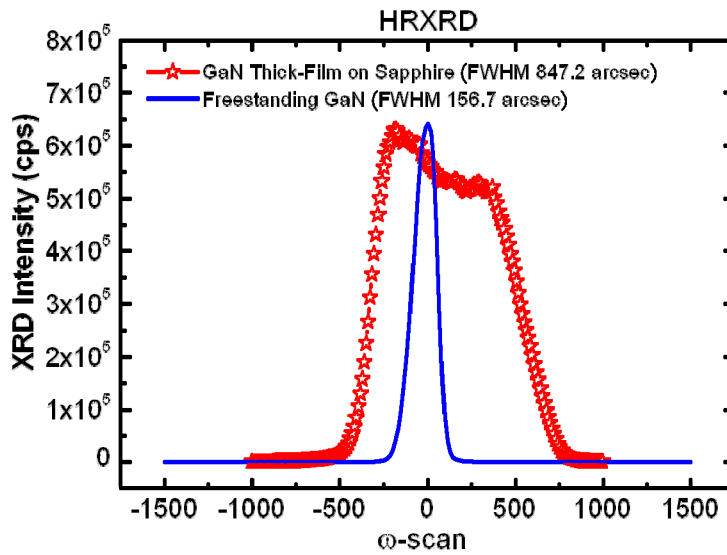


Fig. 12 Rocking curve of HRXRD of GaN grown with a 1.0 °C /min ramping rate before and after laser lift-off process. The FWHM is 156.7 (847.2) arcsec after (before) the laser lift-off process

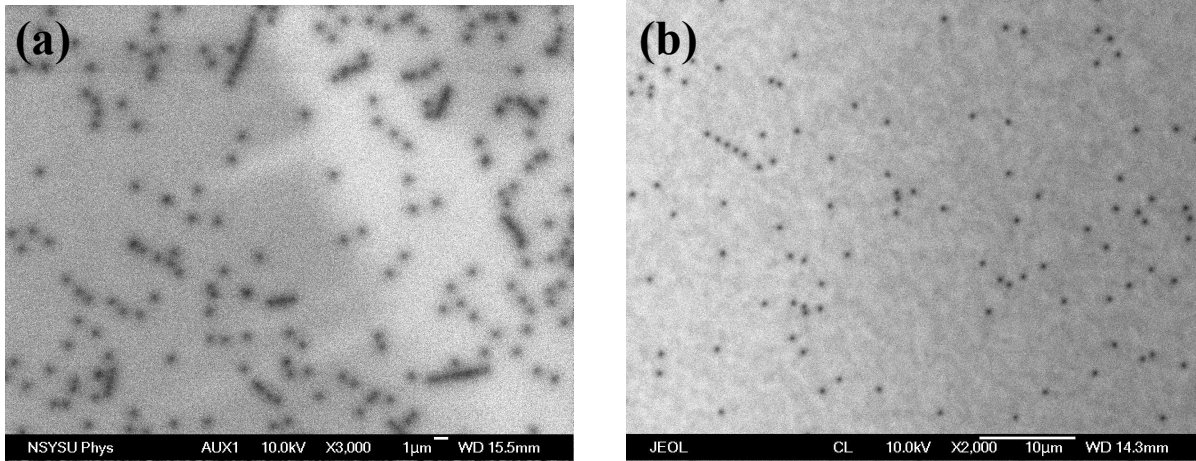


Fig. 13 Top view CL image . (a) 300 μm freestanding GaN wafer. (b) Regrown GaN thick-film with the thickness about 600 μm . The dark spots show the positions of dislocations.

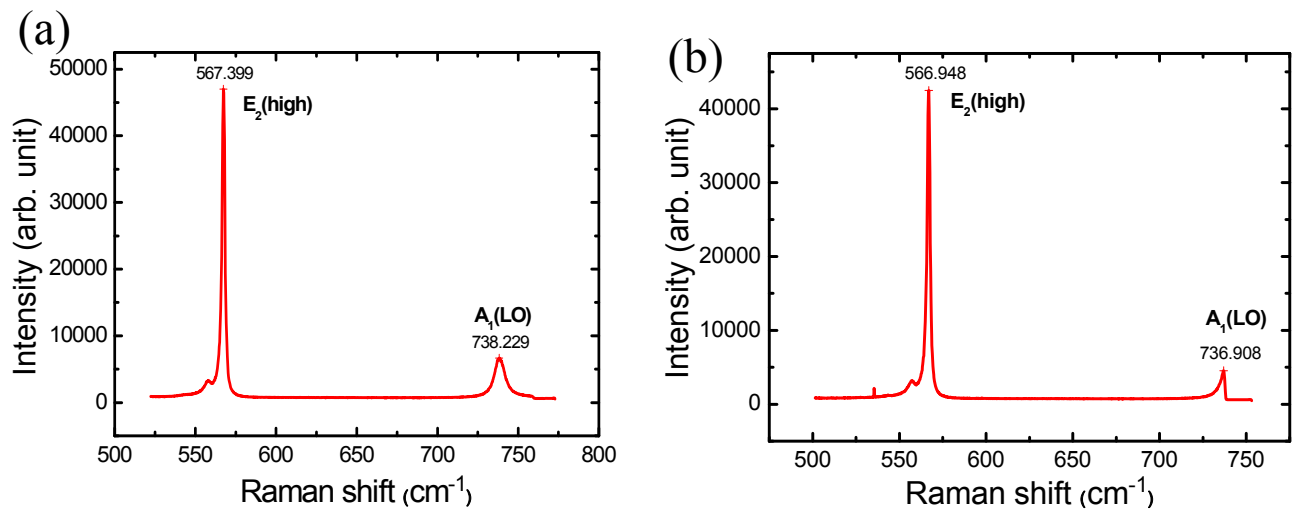


Fig. 14 The plane view Raman spectra of GaN thick-film before (a) and after (b) LLO process.

References

- [1] R. Dwiliński, R. Doradziński, J. Garczyński, L.P. Sierzputowski, A. Puchalski, Y. Kanbara, K. Yagi, H. Minakuchi, H. Hayashi, "Excellent crystallinity of truly bulk ammonothermal GaN," *J. Cryst. Growth* 310, 3911 (2008).
- [2] T. S. Zheleva, S. A. Smith, D. B. Thomson, T. Gehrke, K. J. Linthicum, P. Rajagopal, E. Carlson, W. M. Ashmawi, and R. F. Davis, *MRS Internet J. "Pendeo-Epitaxy - A New Approach for Lateral Growth of GaN Structures"* Nitride Semicond. Res. 4S1, G3.38 (1999).
- [3] N. N. Morgan, Y. Zhizhen, X. "Low-temperature ionic conductivity of the solid solution in the system ZrO_2 - Y_2O_3 - Yb_2O_3 " *Yabou, Materials Science and Engineering B90*,201 (2002).
- [4] B. Beaumont, M. Vaille, G. Natat, A. Bouillé, J. C. Guillaume, P. Vénègues, S. Haffouz, and P. Gibart, *MRS Internet J. "Mg-enhanced lateral overgrowth of GaN on patterned GaN/sapphire substrate by selective Metal Organic Vapor Phase Epitaxy"* Nitride Semicond. Res. 3, 20 (1998).
- [5] Y. Chen, R. Schneider, S. Wang, R. S. Kern, C. H. Chen, and C. P. Kuo, "Dislocation reduction in GaN thin films via lateral overgrowth from trenches" *Appl. Phys. Lett.* 75, 2062 (1999).
- [6] C. Roder, H. Heinke, D. Hommel, T. M. Katona, J. S. Speck, and S. P. Denbaars, " Crystallographic wing tilt in laterally overgrown GaN" *J. Phys. D: Appl. Phys.* 36, A188 (2003).
- [7] I. Kidoguchi, A. Ishibashi, G. Sugahara, and Y. Ban, "Air-bridged lateral epitaxial overgrowth of GaN thin films" *Appl. Phys. Lett.* 76, 3768 (2000).
- [8] I. Kidoguchi, A. Ishibashi, G. Sugahara, A. Tsujimura, and Y. Ban, "Improvement of Crystalline Quality in GaN Films by Air-Bridged Lateral Epitaxial Growth" *Jpn. J. Appl. Phys.* 39, 453(2000).
- [9] A. Ishibashi, Y. Kawaguchi, G. Sugahara, T. Shimamoto, T. Yokogawa, Y. Yamada, Y. Ueki, K. Nakamura, and T. Taguchi, "Spatially resolved cathodoluminescence study on AlGaIn layer fabricated by air-bridged lateral epitaxial growth" *Phys.Stat. Sol. (b)* 241, 2730 (2004).
- [10] S. Bohyama, H. Miyake, K. Hiramatsu, Y. Tsuchida, and T. Maeda, "Freestanding GaN Substrate by Advanced Facet-Controlled Epitaxial Lateral Overgrowth Technique with Masking Side Facets" *Jpn. J. Appl. Phys.* 44, 24 (2005).
- [11] B. Heying, X. H. Wu, S. Keller, Y. Li, D. Kapolnek, B. P. Keller, S. P. Denbaars, and . S. Speck, "Role of threading dislocation structure on the x-ray diffraction peak widths in epitaxial GaN films" *Appl. Phys. Lett.* 68, 643 (1996).
- [12] H. Heinke, V. Kirchner, S. Einfeldt, and D. Hommel, "X-ray diffraction analysis of the defect structure in epitaxial GaN" *Appl. Phys. Lett.* 77, 2145 (2000).
- [13] M. Kuball, M. Benyoucef, B. Beaumont, and P. Gibart, Raman mapping of epitaxial lateral overgrown GaN: Stress at the coalescence boundary" *J. Appl. Phys.* 90, 3656 (2001).
- [14] A. kaschner, A. Hoffmann, C. Thomsen, F. Bertram, T. Riemann, J. Christen, K. Hiramatsu, T. Shibata, and N. Sawaki, "Optical microscopy of electronic and structural properties of epitaxial laterally overgrown GaN" *Appl. Phys. Lett.* 74, 3320 (1999).
- [15] A. R. Goni, H. Siegle, K. Syassen, C. Thomsen, J.-M. Wagner, Effect of pressure on optical phonon modes and transverse effective charges in GaN and AlN" *Phys. Rev. B* 64 , 035205 (2001).
- [16] F. Bertram, T. Riemann, J. Christan, A. Kaschner, A. Hoffmann, K. Horamatsu, T. Shibata, N. Sawaki, "Epitaxial lateral overgrowth of GaN structures: spatially resolved characterization by cathodoluminescence microscopy and micro-Raman spectroscopy" *Materials Science and Engineering B* 59, 117 (1999).
- [17] M. Kuball, M. Benyoucef, B. Beaumont, P. Gibart, "Raman mapping of epitaxial lateral overgrown GaN: Stress at the coalescence boundary" *Jpn. J. Appl. Phys.* 90, 3656 (2001).
- [18] R. D. Vispute, V. Talyansky, S. Choopun, R. P. Sharma, T. Venkatesan, M. He, X. Tang, J. B. Halpern, M. G. Spencer, Y. X. Li, L. G. Salamanca-Riba, A. A. Iliadis, and K. A. Jones: "Heteroepitaxy of ZnO on GaN and its implications for fabrication of hybrid optoelectronic devices" *Appl. Phys. Lett.* 73, 348 (1998).
- [19] S. Hearne, E. Chason, J. Han, J. A. Floro, J. Figiel, J. Hunter, H. Amano, and I. S. T. Tsong: "Stress evolution during metalorganic chemical vapor deposition of GaN" *Appl. Phys. Lett.* 74, 356 (1999).
- [20] T. Detchprohm, K. Hiramatsu, K. Itoh, and I. Akasaki: *Jpn. "Relaxation process of the thermal strain in the GaN/ α Al $_2$ O $_3$ heterostructure and determination of the intrinsic lattice-constants of GaN free from the strain"* *J. Appl. Phys.* 31, L1454 (1992).

- [21] Y. Oshima, T. Eri, M. Shibata, H. Sunakawa, K. Kobayashi, T. Ichihashi, and A. Usui: Jpn. "Preparation of freestanding GaN wafers by hydride vapor phase epitaxy with void-assisted separation" *J. Appl. Phys.* 42, L1 (2003).
- [22] Y. Oshima, T. Suzuki, T. Eri, Y. Kawaguchi, K. Watanabe, M. Shibata, and T. Mishima: "Thermal and optical properties of bulk GaN crystals fabricated through hydride vapor phase epitaxy with void-assisted separation," *J. Appl. Phys.* 98, 103509 (2005).
- [23] S. Bohyama, H. Miyake, K. Hiramatsu, Y. Tsuchida, and T. Maeda: "Freestanding GaN Substrate by Advanced Facet-Controlled Epitaxial Lateral Overgrowth Technique with Masking Side Facets," *Jpn. J. Appl. Phys.* 44, L24 (2005).
- [24] C. Hennig, E. Richter, M. Weyers, and G. Tränkle: "Freestanding 2-in GaN layers using lateral overgrowth with HVPE," *J. Cryst. Growth* 310, 911 (2008).
- [25] M.K. Kelly, R.P. Vaudo, V.M. Phanse, L. Gorgens, O. Ambacher, and M. Stutzmann: "Large Free-Standing GaN Substrates by Hydride Vapor Phase Epitaxy and Laser-Induced Liftoff," *Jpn. J. Appl. Phys.* 38, 217 (1999).
- [26] M. Kelly, O. Ambacher, M. Stutzmann, M. Brandt, R. Dimitrov, and R. Handschuh: "Freestanding GaN-substrates and devices," United States Patent 6,559,075 B1 (2003).
- [27] W.S. Wong, T. Sands, N.W. Cheung, M. Kneissl, D.P. Bour, P. Mei, L.T. Romano, and N.M. Johnson: "Fabrication of thin-film InGaN light-emitting diode membranes by laser lift-off," *Appl. Phys. Lett.* 75, 1360 (1999).
- [28] C. Kisielowski, J. Krüger, S. Ruvimov, T. Suski, J. W. Ager III, E. Jones, Z. Liliental-Weber, M. Rubin, E. R. Weber, M. D. Bremser, and R. F. Davis: "Strain-related phenomena in GaN thin films," *Phys. Rev. B* 54, 17745 (1996).